Technical article

Nonlocal Homogenization

***Abstract* — The proposed theory of nonlocal homogenization applies to periodic structures with arbitrary cell sizes, not necessarily very small relative to the wavelength. The end result is an extended second-order material tensor that includes, in the most general case, the usual 6×6 block of local parameters (permeability, permittivity and magnetoelectric coupling) and an additional block that rigorously quantifies nonlocality. The local part of the tensor relates the mean values of pairs of coarse-grained fields, while the nonlocal part relates the mean values to *variations* of the fields. The theory is minimalistic, with only two fundamental premises at its core: (i) the coarse-grained fields satisfy Maxwell's equations and boundary conditions exactly; and (ii) the material tensor is a linear relationship between the pairs of coarse-grained fields. Nontrivial magnetic behavior of intrinsically dielectric media is a logical consequence of the theory. The approximations involved and the respective errors are clearly identified. Illustrative examples of resonant structures with high-permittivity inclusions are given.**

The theory is closely related to multiple subjects of direct interest to the Compumag community: edge and face elements, discrete Hodge operators, hierarchical bases, applications to electromagnetic metamaterials and to laminated cores of electrical machines.

To the memory of J. Douglas Lavers

I Introduction: Effective Medium Theory Meets Compumag

Effective medium theory – the derivation of equivalent macroscopic parameters of a composite material from its microstructure – is a very broad and well established area, with a long history. In physics, it dates back to the work of Mossotti (1850), Lorenz (1869), Lorentz (1878), Clausius (1879), and Maxwell Garnett (1904). A number of more advanced physical theories followed, of which most relevant to electromagnetics are various extensions of the Maxwell Garnett formula to wave problems: by Lewin (1947), Khizhnyak (1957–59), Waterman & Pedersen (1986) [40, 35, 36, 76]. In particular, Khizhnyak made an interesting observation that "an artificial dielectric ... made from inherently nonmagnetic materials, at higher frequency ... will exhibit both dielectric and magnetic anisotropy;" see [49] for an interesting summary of these developments. Modern physical theories of homogenization are presented in Choy's monograph [12], with the emphasis on random rather than periodic media.

The mathematical literature on the subject is also rich and includes the monographs by Bakhvalov & Panasenko, Bensoussan *et al.*, Oleinik and her collaborators, Dal Maso, Sanchez-Palencia and Tartar [4, 5, 33, 15, 55, 66]. A very interesting subproblem is to determine the lower and upper bounds on the effective parameters of composite materials with given constituents and to find the microstructures that actually attain these bounds; see Milton's monograph [46].

Many purely numerical approaches to homogenization have also been put forward within the multiscale framework that has progressed from multigrid / multilevel methods in the 1960s–1980s to multiphysics over the last decade. This numerical perspective is beyond the scope of this paper; the interested reader is referred to the review paper [17] by E *et al.* and to [22, 31, 32, 38, 50] and references there.

Altogether, according to the ISI database, there are currently about 24,000 papers on effective medium theory / homogenization, covering mathematical, physical, numerical and engineering aspects of this subject. Why, then, yet another paper? What else needs to be done and why would that be of interest to the Compumag community?

The existing theories, for the most part, operate in the *homogenization limit*, when the cell size of the microstructure (or other similar parameters) tends to zero. This is sufficient for many applications, but not for all. One notable exception is optical metamaterials – artificial periodic structures judiciously designed to control the propagation of electromagnetic waves and to achieve remarkable effects such as high-frequency magnetism nonexistent in natural materials. If the zero-cell-size limit is taken, magnetism (and negative refraction, an even more remarkable phenomenon) disappear; the material behavior becomes rather trivial. This conclusion has been reached independently by several researchers who have approached the subject from very different perspective [8, 45, 62, 70].

Thus an extension of existing theories beyond the homogenization limit is desirable. I call such an extension "nonlocal homogenization," for reasons that will become more clear further on. The nonlocality implies that the mean values of the $\mathbf{D}, \mathbf{B}$ fields depend not only on the mean values but also on the *variations* (derivatives) of the $\mathbf{E}, \mathbf{H}$ fields. In addition to electromagnetic analysis of optical metamaterials, nonlocal homogenization may be relevant for the laminated cores of electrical machines, especially if the skin depth in the iron sheets is comparable with the thickness of these sheets [13, 27].

Important as these applications are, they may not be the primary reason why the Compumag community may be interested in nonlocal homogenization. A more significant point is that the theory of this paper draws heavily on div- and curl-conforming interpolation, the cornerstone of edge and face element analysis [7]. Here, however, these ideas are used in a new context, analytical in its essence rather than numerical. Despite its connection with the differential-geometric treatment of electromagnetic fields and with discrete Hodge operators [7, 28, 37, 67], the theory is framed in terms of classical vector calculus more familiar to the majority of engineers and physicists.

Notable for the Compumag is also a link of the proposed theory to Model Order Reduction methods developed by Dyczij-Edlinger and others [57].

While the methodology of this paper is itself semi-

analytical, its usage will call for new numerical tools and procedures – yet another significant Compumag connection. In general, nonlocal models are computationally costly and should be employed with a great deal of caution. In the case under consideration, however, such models may well be warranted and recommended. One reason is that the nonlocality can typically be expected to be weak – the $\mathbf{D}, \mathbf{B}$ fields will depend on $\mathbf{E}, \mathbf{H}$ not in the whole computational domain but in a small volume around any given point in the medium. Secondly, as already noted, there are application problems where the local model is simply unavailable or inaccurate. Then the choice is not between a local and a nonlocal model (in which case the local one would clearly be preferable) but between a nonlocal model and a full-scale solution of Maxwell's equations in the microstructure. The latter in most practical cases is just not feasible.

In this paper, nonlocal effects are described via the variations (derivatives) of the $\mathbf{E}, \mathbf{H}$ fields within the lattice cell. One undesirable consequence of that is an increased order of the resulting differential equations. A possible alternative is to convert the model into an integrodifferential form, with the nonlocality represented by a suitable integral kernel. Methods of this kind are currently under development but are not covered in this paper. The immediate focus here is on the analytical treatment of nonlocal effects; numerical ramifications will be considered in future research.

The proposed theory of nonlocal homogenization yields an extended second-order material tensor that contains not only the usual 6×6 matrix of local material parameters (in 3D electrodynamics), but also an additional block quantifying nonlocality rigorously. The local part of the tensor relates the mean values of the coarse-grained fields, while the nonlocal part relates these mean values to *variations* of the fields.

II Proposed Theory: Key Concepts

The complex electromagnetic behavior of metamaterials – artificial periodic structures with features smaller than the vacuum wavelength – has been extensively investigated over the last decade. Effective medium description of such structures is indispensable for their analysis and design, and the existing literature on this subject is quite vast. The approaches include retrieval via S-parameters, applications and extensions of classical mixing formulas for small inclusions, analysis of dipole lattices, special current-driven models, and much more. Reviews and references are available in [56]–[61]; see also [64, 72]. One particularly intriguing phenomenon is "artificial magnetism" at high frequencies. A physical explanation of it is that resonating elements in metamaterial cells act as elementary magnetic dipoles. However, there is a paradox associated with such magnetism. In a metamaterial composed of intrinsically nonmagentic components, the "microscopic" magnetic fields $\mathbf{h}$ and $\mathbf{b}$ are the same; yet somehow their spatial averages – the respective coarse-grained fields $\mathbf{H}$ and $\mathbf{B}$ – differ. How can two identical quantities give rise to two different averages?

Remark. Here and in the remainder of the paper I use the Gaussian system of units, partly to avoid the nuisance of μ_0 appearing everywhere and partly for consistency with the literature on metamaterials, the majority of which is written in the Gaussian system.

Our point of departure is the traditional formulation of Maxwell's equations in terms of four "microscopic" (pointwise) fields $\mathbf{e}, \mathbf{d}, \mathbf{h}, \mathbf{b}$; their coarse-grained counterparts $\mathbf{E}, \mathbf{D}, \mathbf{H}, \mathbf{B}$ need to be properly defined. Alternative formulations with fewer fields are available, due most notably to Agranovich, Ginzburg, Landau & Lifshitz [1, 39, 60]. The four-field formulation, however, is universally accepted in engineering (including, certainly, Compumag) and widely used in applied physics due to a number of advantages. It treats intrinsic magnetism, when it exists (at low frequencies), in a very natural way; it avoids *unnecessary* nonlocality; it yields simple local boundary conditions without additional surface currents.

Besides, there is a certain elegance in treating two pairs of fields in a symmetric fashion [7]. If so, it is quite natural to wonder why *the same* averaging procedure should not be applied to all four microscopic fields, in which case the paradox noted above arises: no magnetic effects despite the overwhelming evidence to the contrary (all references on metamaterials cited above deal with magnetism in one way or another; see also [9]).

The theory of [72] and this paper resolves this paradox. For Maxwell's equations and standard boundary conditions to be honored, the coarse-grained fields $\mathbf{H}$ and $\mathbf{B}$ must be obtained from the microscopic $\mathbf{h}$ and $\mathbf{b}$ via *different* procedures. Indeed, $\mathbf{H}$ has tangential continuity across all interfaces, whereas $\mathbf{B}$ has normal continuity. Specific interpolation procedures producing fields with the required types of continuity are discussed in [72]; see also Section III.

The proposed theory has several distinguishing features:

- The material is characterized by an extended parameter matrix with the usual 6×6 diagonal block and an off-diagonal block that quantifies nonlocality. This generalizes the traditional local treatment.
- The procedure is applicable to any cell size, not necessarily very small relative to the wavelength.
- The methodology is based on a *direct* field analysis in a single lattice cell, in contrast with S-parameter retrieval procedures [10, 11, 63] where the effective parameters are inferred from reflection and transmission coefficients of a metamaterial slab.
- There are no adjustable or fitting parameters and no artificial averaging rules contrived to arrive at a desired result such as magnetic permeability $\mu \neq 1$. Nontrivial magnetic behavior, if present, follows logically from the method.
- The coarse-grained fields are defined to satisfy Maxwell's equations and interface boundary conditions exactly.
- The method can take advantage of any available analytical, semi-analytical and/or numerical approximations of the electromagnetic field in a given lattice cell.
- The approximations made and the respective errors are clearly and explicitly identified and quantified not only in the asymptotic "big-$\mathcal{O}$" sense but numerically as well.
- The model of nonlocality resulting from the theory can be incorporated into existing methods and software for field simulation. However, this subject is beyond the scope of the present paper and will be taken up elsewhere.

- The theory is minimalistic, with only a few fundamental premises at its core; see Section II.

Of a very large number of homogenization methods in the existing literature, two need to be mentioned separately: one due to its very wide acceptance and the other one due to its special relevance to the present paper. In one most common procedure, effective parameters of a metamaterial slab are "retrieved" from transmission/reflection data (i.e. from S-parameters). Being essentially an inverse problem, this parameter retrieval has some inherent ill-posedness that manifests itself in the multiplicity of solutions, due to the ambiguity of branches of the inverse trigonometric functions involved. Parameters retrieved for slabs of varying thickness (let alone shape) are not always consistent. More fundamentally, the retrieval procedure does not by itself explain why such consistency *should* be expected; obviously, there must be an underlying reason for it. That deeper reason is the definition of parameters as relations between the (pairs of) coarse-grained fields within the material.

The existing approach most closely related to the methodology of the present paper is due to the insight of Smith & Pendry, who suggested different averaging procedures for different fields in the cell [64]. This idea, subsequently elaborated in [42], stems from the analogy with finite difference schemes on staggered grids. The present paper, along with [72], provides an expanded and substantially more rigorous foundation for this physical insight, as well as a much more comprehensive description of the behavior of the fields in terms of the extended material tensor comprising local and nonlocal parameters. The exposition below starts with a general description of the key concepts, followed by some technical details, implementation and examples.

Since material parameters are linear relations between the coarse-grained fields, a natural plan is to define these fields unambiguously and then establish a proper linear mapping between the $(\mathbf{H}, \mathbf{E})$ and $(\mathbf{B}, \mathbf{D})$ pairs.

The motivation for any effective medium theory is that the microscopic fields vary too rapidly to be easily described and analyzed; one may say that they have "too many degrees of freedom" (d.o.f.). An obvious idea is to split them up into coarse-grained (capital letters) and fast (tilde-letters) components, e.g. $\mathbf{b} = \mathbf{B} + \mathbf{b}^{\sim}$. For reasons explained in detail below, this splitting should satisfy several conditions:

1. By definition, the coarse-grained fields must vary much less rapidly than the total fields. Nevertheless the former must approximate the latter, in a certain well defined sense, everywhere in space.

2. The coarse-grained fields must satisfy Maxwell's equations and interface boundary conditions.

3. The fast and coarse components must be semi-decoupled. That is, the fast components may depend on the coarse ones, but the coarse fields must not depend, or may depend only very weakly, on the fast ones.

4. There exists a linear relation (map) between the pairs of coarse-grained fields $(\mathbf{E}, \mathbf{H})$ and $(\mathbf{D}, \mathbf{B})$ that is independent of the incident waves (at least to a given level of approximation).

The requirements above define not a single method but a *framework* from which conceptually similar but not fully equivalent homogenization methods could potentially be obtained by making these requirements more specific.

The rationale for each of the conditions above is as follows. The first one represents, from the physical perspective, the very essence of homogenization. From a more mathematical viewpoint of analysis and simulation, one might accept a weaker requirement that the coarse fields could be described with much fewer degrees of freedom but would not necessarily have to vary less rapidly than the total fields. For example, the field in a periodic structure can in many cases be described by a very limited number of Bloch waves with judiciously chosen wave vectors (see e.g. [57] for some illuminating examples); this fact may be effectively used in semi-analytical and numerical methods such as Generalized Finite Element Method (GFEM) [2, 3, 53], Discontinuous Galerkin methods [29], and Flexible Local Approximation MEthods (FLAME) [68, 69, 71]. Nevertheless the focus of this paper is on physical, not numerical, methods.

Pointwise approximation of the miscorscopic fields by the coarse ones is in general not feasible and not required, as rapid local field oscillations due to the resonance effects in metamaterial cells are definitely of interest. Instead, we assume that the coarse-grained fields are close to the real ones at the cell boundary, where the fields vary more smoothly. Inside the cell, the coarse-grained fields are defined by interpolation from the boundary values.

Although the second requirement (coarse-grained fields satisfying Maxwell's equations) seems to be self-evident, many existing methods pay surprisingly little attention to it and may actually violate it. In particular, coarse fields defined via simple volume averaging do not satisfy Maxwell's boundary conditions. We shall return to this important point later.

The rationale for the third requirement (weak coupling) is that, if both components were to be coupled strongly, the two-scale problem would not be any simpler than the original one involving the total field.

The fourth requirement is for now open-ended and needs to be made more specific. Let us assume that, for a given microscopic field $(\mathbf{e}, \mathbf{d}, \mathbf{b})$, the coarse-grained fields $(\mathbf{E}, \mathbf{D}, \mathbf{B}, \mathbf{H})$ satisfying conditions 1–3 above have been defined in some way. The central question then is to relate the pairs of coarse-grained fields. The generalized "material parameter" is, mathematically, a linear map $\mathcal{L} : (\mathbf{E}, \mathbf{H}) \to (\mathbf{D}, \mathbf{B})$ from the functional space of fields $(\mathbf{E}, \mathbf{H})$ to the functional space of $(\mathbf{D}, \mathbf{B})$. The dimensionality of this map depends on the coarse-grained interpolations chosen. A high-dimensional linear map could be of use in numerical procedures but does not offer much physical insight. One critical question then is whether a good *low-dimensional* approximation of this linear map can be found. A formal linear-algebraic answer to this question is well known: the best approximation of a given rectangular matrix by a matrix of rank m is via the highest m singular values and the respective singular vectors (see e.g. [25] or [16] for the mathematical details). The error of this approximation is equal to the $m+1$st singular value. One may note a conceptual similarity with the well known Principal Component Analysis (PCA); see e.g. [58] for an elementary tutorial.

Although the PCA perspective is instructive, it does not provide a direct connection with the physical parameters

such as ϵ or μ. Our objective is still to find new bases in which the material map $\mathcal{L}$ could be approximately "compressed" to a low-dimensional form, but the bases we are seeking are physical rather than formally algebraic. More specifically, in this physical basis the first few components of the coarse-grained fields $\mathbf{E}, \mathbf{H}, \mathbf{D}, \mathbf{B}$ are to be their mean values, and the subsequent components – the deviations from the mean. Such bases and the respective matrix representation of the map $\mathcal{L}$ will be called *canonical* and are described in Section III in detail.

III Proposed Theory: Details

A Equations

Consider a periodic structure composed of materials that are assumed to be (i) intrinsically nonmagnetic (which is true at sufficiently high frequencies [39]); (ii) satisfy a linear local constitutive relation $\mathbf{d} = \epsilon\mathbf{e}$. For simplicity, we assume a cubic lattice with cells of size a. Maxwell's equations for the microscopic fields are, in the frequency domain and with the $\exp(-\mathrm{i}\omega t)$ phasor convention,

$$\nabla \times \mathbf{e} = \mathrm{i}\omega c^{-1}\mathbf{b}, \quad \nabla \times \mathbf{b} = -\mathrm{i}\omega c^{-1}\mathbf{d}$$

As a reminder, the Gaussian system of units is used throughout the paper, and small letters $\mathbf{b}, \mathbf{e}, \mathbf{d}$, etc., denote the "microscopic" – i.e. true physical – fields that in general vary rapidly in space (but still on the scale $\gtrapprox 10$ nm, so that the intrinsic permittivity is physically meaningful). Capital letters refer to smoother fields that vary on the scale coarser than the lattice cell size.

These coarse-grained fields **B**, **H**, **E**, **D** must be defined in such a way that the boundary conditions be honored. Simple cell-averaging does not satisfy this condition [72]. To understand why, consider, say, the "microscopic" magnetic field, for simplicity just a function of one coordinate, $\mathbf{b}(x)$, at a material/air interface $x = 0$. For intrinsically nonmagnetic media, this field is continuous across the interface, i.e. $\mathbf{b}(0-) = \mathbf{b}(0+)$. Since the field fluctuates in the material, there is no reason for its value at $x = 0+$ to be equal to its cell average over $0 \le x \le a$, except by coincidence. Thus, if this cell average is used to define the **B** field, its normal component at the interface will almost always be discontinuous, which is nonphysical. Likewise, if the **H** field is defined via the cell average, its tangential component will in general behave in a nonphysical way.

As a rough, "zero-order," approximation, these nonphysical field jumps across interfaces could be neglected. This may indeed be possible in the absence of resonances or for vanishingly small cell sizes. However, neglecting strong field fluctuations in other cases would eliminate the very resonance effects that we wish to capture.

The general stages of the method are shown in Fig. 1. The field in the lattice cell is approximated with a superposition of several modes (e.g. Bloch waves in the periodic case). Each of these modes is then "coarse grained" by two complementary interpolation procedures, div-conforming for the $(\mathbf{D}, \mathbf{B})$ fields and curl-conforming for $(\mathbf{E}, \mathbf{H})$ (Section B). The extended material tensor is then found as a linear map between these field pairs.

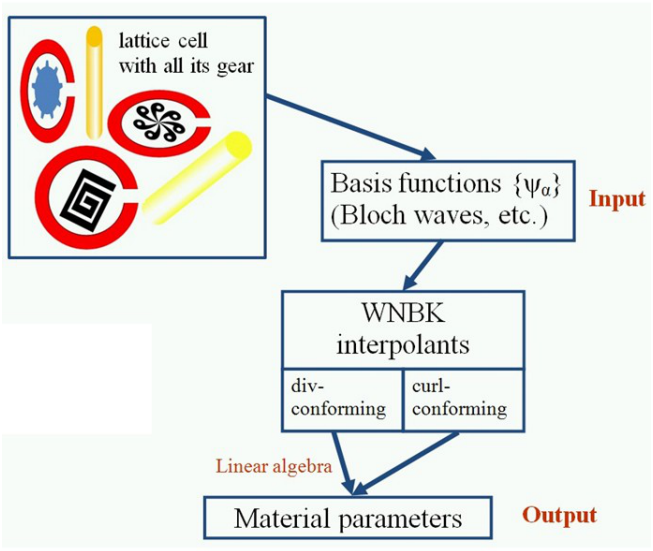

Figure 1: Key parts of the proposed methodology. Two types of interpolation are used to obtain the coarse-grained fields with tangential and normal continuity. The electromagnetic field inside the cell, with all its microstructure, is approximated as a superposition of basis modes. Material parameters are linear relationships between the pairs of coarse-grained fields.

B Coarse-grained Fields: Interpolation and Continuity Conditions

This is a key point, where we depart from more traditional methods of field averaging. The coarse-grained **E** and **H** fields are produced from the "microscopic" ones, **e** and **b**, by an interpolation that respects tangential continuity across all interfaces. The coarse-grained **D** and **B** fields are produced from **d** and **b** by another interpolation, one that preserves normal continuity. For the Compumag community, these interpolation procedures are quite natural and date back to van Welij's 1985 paper [74] and the seminal work by Whitney, Nedelec [51, 52], Kotiuga and Bossavit [6, 7, 37]. Here, this interpolation is considered in a very different context – nonlocal homogenization.

Tangentially continuous interpolation is effected by vectorial functions like the one shown in Fig. 2, in a 2D rendition for simplicity. The circulation of this function is equal to one along one edge (in the figure, the vertical edge shared by two adjacent lattice cells) and zero along all other edges of the lattice.

To shorten all interpolation-related expressions, *in this section the lattice cell is normalized to the unit cube* $[0,1]^3$, i.e. $a = 1$. Then a formal expression for four x-directed functions **w** is [74]

$$\mathbf{w}_{1-4} = 2\hat{x}\{yz, (1-y)z, y(1-z), (1-y)(1-z)\} \qquad (1)$$

Another eight functions of this kind are obtained by the cyclic permutation of coordinates in the expression above. For each lattice cell, there are 12 such interpolating functions altogether (one per edge). Each function $\mathbf{w}_\alpha$ has unit circulation along edge α ($\alpha = 1, 2, \ldots 12$) and zero circulations along all other edges. All of them are vectorial interpolating functions, bilinear with respect to the spatial coordinates. (In [72] these functions were defined in the

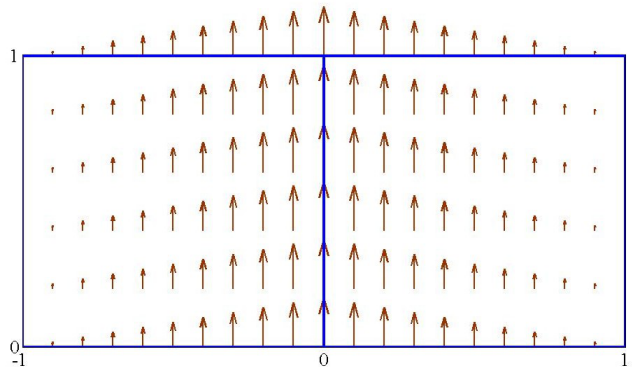

Figure 2: (From [72].) A 2D analog of the vectorial interpolation function $\mathbf{w}_\alpha$ (in this case, associated with the central vertical edge shared by two adjacent cells). Tangential continuity of this function is evident from the arrow plot; its circulation is equal to one over the central edge and to zero over all other edges.

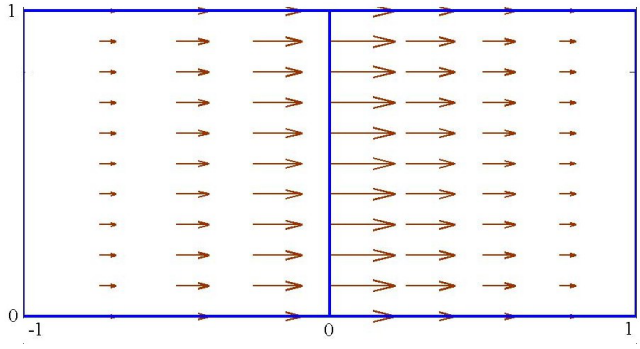

Figure 3: (From [72].) A 2D analog of the vectorial interpolation function $\mathbf{v}_\beta$ (in this case, associated with the central vertical edge). Normal continuity of this function is evident from the arrow plot; its flux is equal to one over the central edge and zero over all other edges.

cell scaled to $[-1,1]^3$ rather than to $[0,1]^3$, and therefore the algebraic expressions differ.)

The coarse-grained $\mathbf{E}$ and $\mathbf{H}$ fields can then be represented by interpolation from the edges into the volume of the cell as follows:

$$\mathbf{E} \;=\; \sum\nolimits_{\alpha=1}^{12} [\mathbf{e}]_\alpha \mathbf{w}_\alpha, \quad \mathbf{H} \;=\; \sum\nolimits_{\alpha=1}^{12} [\mathbf{b}]_\alpha \mathbf{w}_\alpha \qquad (2)$$

where $[\mathbf{e}]_\alpha = \int_\alpha \mathbf{e}\cdot\mathbf{dl}$ is the circulation of the (microscopic) $\mathbf{e}$-field along edge α; similarly for $[\mathbf{b}]_\alpha$. In the calculation of the circulations, integration along the edge is always assumed to be in the positive direction of the respective coordinate axis.

Now consider the second kind of interpolation that preserves the normal continuity and produces the $\mathbf{D},\mathbf{B}$ fields from $\mathbf{d}$ and $\mathbf{b}$. A typical interpolating function (2D rendition again for simplicity) is shown in Fig. 3. The flux of this function through a face shared by two adjacent cells is equal to one; the flux through all other faces is zero. Two such functions in the x-direction are (as before, for the cell size normalized to unity) [74]

$$\mathbf{v}_{1-2} = \hat{x}\{x, 1-x\}$$

and another four functions $\mathbf{v}_{3-6}$, in the y- and z-directions, are expressed similarly. These six functions can be used to define the coarse-grained $\mathbf{D}$ and $\mathbf{B}$ fields by interpolation from the six faces into the volume of the unit cell:

$$\mathbf{D} \;=\; \sum_{\beta=1}^{6} [[d]]_\beta \mathbf{v}_\beta, \quad \mathbf{B} \;=\; \sum_{\beta=1}^{6} [[b]]_\beta \mathbf{v}_\beta, \qquad (3)$$

where $[[d]]_\beta \;=\; \int_\beta \mathbf{d}\cdot\mathbf{dS}$ is the flux of $\mathbf{d}$ through face β ($\beta = 1,2,\ldots,6$); similar for the $\mathbf{b}$ field. In the calculation of fluxes, it is convenient to take the normal to any face in the positive direction of the respective coordinate axis (rather than in the outward direction).

The coarse-grained $\mathbf{E}$ and $\mathbf{H}$ fields so defined have 12 degrees of freedom in any given lattice cell – mathematically, they lie in the 12-dimensional functional space spanned by functions $\mathbf{w}_\alpha$. This space was denoted with $W_{\rm curl}$ in [72]: the 'W' honors Whitney [78] and 'curl' indicates fields whose curl is a regular function rather than a general distribution. This implies, in physical terms, the absence of equivalent surface currents and the tangential continuity of the fields involved.

Similarly, $\mathbf{D}$ and $\mathbf{B}$ within any lattice cell lie in the six-dimensional functional space $W_{\rm div}$ spanned by functions $\mathbf{v}_\beta$. Importantly, it can be shown that the div- and curl-spaces are compatible in the following sense:

$$\nabla \times W_{\rm curl} \subset W_{\rm div} \qquad (4)$$

That is, the curl of any function from $W_{\rm curl}$ (i.e. the curl of any coarse-grained field $\mathbf{E}$ or $\mathbf{H}$ defined by (2)) lies in $W_{\rm div}$. Because of this compatibility of interpolations, the coarse-grained fields satisfy Maxwell's equations exactly [72]:

$$\nabla\times\mathbf{E} \;=\; \mathrm{i}\omega c^{-1}\mathbf{B}; \quad \nabla\times\mathbf{H} \;=\; -\mathrm{i}\omega c^{-1}\mathbf{D} \qquad (5)$$

By construction, they also satisfy the proper continuity conditions at all interfaces.

To recap the ideas, Fig. 4 schematically illustrates the interpolation procedures and the linear-algebraic part of the proposed method. The simplified 1D rendition shows only the x axis, the tangential (y,z) components of $\mathbf{E},\mathbf{H}$ and the normal (x) component of $\mathbf{D},\mathbf{B}$. Other components (not shown) may be discontinuous at cell boundaries and at material interfaces. The linear operator $\mathcal{L}$ relating the pairs of coarse-grained fields is in general multidimensional, commensurate with the dimensions of the interpolation spaces chosen. As we shall see, $\mathcal{L}$ has a 6×6 (or smaller) matrix block in a suitable "canonical" (hierarchical) basis; this block relates the field averages of $(\mathbf{D},\mathbf{B})$ to the field averages of $(\mathbf{E},\mathbf{H})$. The remainder of the matrix relates the field averages to field *variations* over the cell and can be viewed as a manifestation of nonlocality (see Section IV for further details).

C Approximating Functions

The actual microscopic fields in the material are in general not known and need to be approximated by introducing suitable basis functions [72]. Examples include Bloch waves in the periodic case, plane waves, cylindrical or spherical harmonics, etc. For a non-vanishing cell size, the field has an infinite number of degrees of freedom; thus, as a matter of principle, its representation in a finite basis is approximate. Nevertheless the relevant behavior of the fields can be captured very well by relatively small bases [57]. By expanding the bases, one can increase the accuracy of the

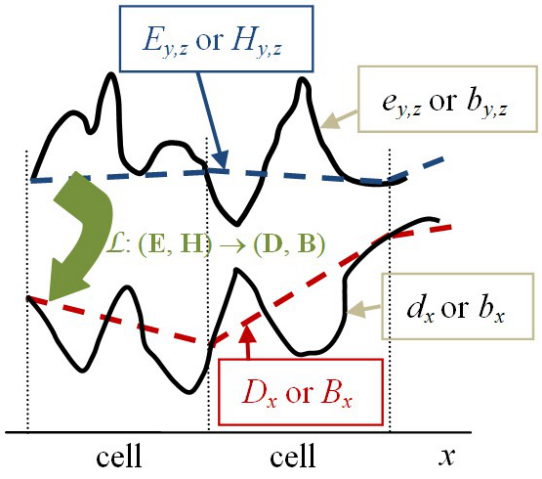

Figure 4: (From [73]). A linear relation between the coarse-grained fields. $\mathbf{E}, \mathbf{H}$ are interpolated to ensure tangential continuity; $\mathbf{D}, \mathbf{B}$ are normally continuous. 1D rendition for simplicity. In a canonical basis, the multidimensional operator $\mathcal{L}$ contains a 6×6 submatrix of local electrodynamic parameters.

representation of the fields, at the expense of higher complexity. A small number of degrees of freedom corresponds to local material parameters, a moderately higher number – to nonlocal ones, and a large number falls under the umbrella of numerical simulation. This viewpoint *unifies local, nonlocal and numerical treatment* of electromagnetic characteristics of metamaterials.

In the periodic case, the most natural basis modes are Bloch waves traveling in different directions (the approximation accuracy in general depends on the number of basis modes chosen). If the structure is not necessarily periodic, one may note that tangential components of the electric or, alternatively, magnetic field on the cell boundary define the field inside the cell uniquely, except for the special cases of interior resonances. To specify the basis, it is thus sufficient to consider the boundary values in lieu of the values inside of the cell. A natural set of approximating functions can thus be obtained by setting the tangential components of $\mathbf{E}$ or $\mathbf{H}$ on the cell boundary as low order polynomials and using that as Dirichlet conditions for Maxwell's equations within the cell. This alternative to Bloch modes will be explored in more detail in subsequent communications.

More formally, let the electromagnetic field be approximated as a linear combination of some basis waves (modes) ψ_α [72]:

$$\Psi^{eh} = \sum\nolimits_\alpha c_\alpha \psi_\alpha^{eh} + \delta^{eh}; \quad \Psi^{db} = \sum\nolimits_\alpha c_\alpha \psi_\alpha^{db} + \delta^{db} \quad (6)$$

In the general case, Ψ and all ψ_α are six-component vector comprising both microscopic fields; e.g. $\Psi^{eh} \equiv \{\Psi^e, \Psi^h\}$, etc. The δs are approximation errors that will tend to decrease as more modes are included in the expansion. For simplicity of further analysis, we assume that the chosen set of modes is rich enough, so that the approximation errors are small.

D The Hierarchical ("Canonical") Basis

By construction of the coarse-grained interpolants, the $\mathbf{E}$ and $\mathbf{H}$ fields, taken together within a lattice cell, lie in a 24-dimensional linear space (12 edge-based degrees of freedom for each field), while the $\mathbf{D}$ and $\mathbf{B}$ fields together lie in a 12-dimensional space (six face-based d.o.f. for each field). Therefore a linear relationship between these pairs of fields is, technically, a map from a complex 24-dimensional space to a 12-dimensional one. For a given pair of bases in these spaces, this map is described by a 24×12 complex matrix and can be viewed as a generalized material tensor. However, there is an important caveat and a necessary amendment.

The caveat is that there exist linear relationships between the above-mentioned degrees of freedom that follow directly from Maxwell's equations, regardless of the content of the lattice cell. For example, Faraday's law relates the edge circulations of the electric field over any face of the cell and the magnetic flux through the same face.

Such Maxwell dependencies need to be eliminated before the generalized material tensor is sought. This could be done in a formal linear-algebraic way, but our preference is to stay closely connected to the physics. With this in mind, a natural, "canonical," set of degrees of freedom is as follows:

Boundary averages of the coarse fields, i.e. $\langle \mathbf{E} \times \mathbf{n} \rangle_{\partial\Omega}$, $\langle \mathbf{H} \times \mathbf{n} \rangle_{\partial\Omega}$, $\langle \mathbf{n}(\mathbf{D} \cdot \mathbf{n}) \rangle_{\partial\Omega}$, $\langle \mathbf{n}(\mathbf{B} \cdot \mathbf{n}) \rangle_{\partial\Omega}$. To reiterate, it is the tangential components of $\mathbf{E}$, $\mathbf{H}$ and the normal components of $\mathbf{D}$, $\mathbf{B}$ that are being averaged. The coarse-grained fields inside the cell are produced by low-order Whitney-like interpolation of the boundary values, and it is easier to use boundary averages of these fields as a proxy for their volume averages. There are six d.o.f. in this category altogether for the $(\mathbf{E}, \mathbf{H})$ pair (three Cartesian components for each mean field) and six d.o.f. for the $(\mathbf{D}, \mathbf{B})$ pair.

Boundary averages of a *subset* of first partial derivatives of $(\mathbf{E}, \mathbf{H})$: $\langle \partial E_x/\partial y \rangle$, $\langle \partial E_y/\partial z \rangle$, $\langle \partial E_z/\partial x \rangle$, and similarly for $\mathbf{H}$.

Boundary averages of a *subset* of second partial derivatives of $(\mathbf{E}, \mathbf{H})$.

Several comments are in order with regard to this choice of d.o.f.

1. We are generally interested in expressing the mean values of $(\mathbf{D}, \mathbf{B})$, but not their derivatives, in terms of $(\mathbf{E}, \mathbf{H})$ and (if necessary) of the variations of $(\mathbf{E}, \mathbf{H})$ within the cell. Hence the derivatives of $(\mathbf{E}, \mathbf{H})$ *are* included into consideration, while those of $(\mathbf{D}, \mathbf{B})$ do not have to be.

2. The d.o.f. cannot simultaneously contain, say, $\langle \partial E_x/\partial y \rangle$ and $\langle \partial E_y/\partial x \rangle$, because their difference constitutes $\langle \nabla \times \mathbf{E} \rangle_z$ and is directly related to B_z via Faraday's law regardless of the content of the lattice cell. However, it is possible to use linear combinations independent of the curl and symmetrize the derivatives: $\langle \partial E_x/\partial y + \partial E_y/\partial x \rangle$, etc.

3. Considerations regarding the second derivatives are similar but more involved. In particular, the Laplacian of the field on the cell boundary is related, via the wave equation, to the field itself. Thus including all second derivatives in the set of d.o.f. is in general redundant.

4. It is clear from the above that the choice of the additional "nonlocal" d.o.f. is not unique. Different choices

will lead to methods that are conceptually similar but differ in the particular ways of representing and quantifying nonlocality. Thus we have a spectrum of methods – a framework – rather than a single method.

5. Some d.o.f. may vanish due to symmetry. For example, if the lattice cell is symmetric with respect to x, the x-derivatives of the fields need not be included in the basis set.

E The Generalized Material Tensor

We are now in a position to describe the algorithmic stages for obtaining the generalized material tensor:

1. Choose a set of N approximating modes and compute these modes using any analytical, semi-analytical or numerical tools available.

2. Choose a set of M^{EH} and M^{DB} degrees of freedom for the $(\mathbf{E}, \mathbf{H})$ and $(\mathbf{D}, \mathbf{B})$ pairs, respectively, as described in the previous subsection. The d.o.f. will include the mean values of the tangential components of $\mathbf{E}, \mathbf{H}$ and of the normal components of $\mathbf{D}, \mathbf{B}$. In addition, the mean values of some derivatives of $\mathbf{E}, \mathbf{H}$ may be included. By increasing the number of d.o.f.s, one trades higher accuracy for a greater level of nonlocality in the characterization of the material. Typically for 3D problems, $M^{DB} = 6$ (three mean values for each of the two fields) but $M^{EH} \geq 6$ (nonlocal d.o.f.s may be included in addition to the mean values).

3. For each mode $m = 1, 2, \ldots M$, compute its respective degrees of freedom (the mean boundary values of the tangential components of $\mathbf{E}, \mathbf{H}$ for this mode, etc.) Assemble the d.o.f.s for the $\mathbf{E}, \mathbf{H}$ fields into the mth column of matrix W^{EH} and the d.o.f.s for the $\mathbf{D}, \mathbf{B}$ fields into the mth column of matrix W^{DB}. Ultimately, matrix W^{EH} is of dimension $M^{EH} \times N$ and matrix W^{DB} is $M^{DB} \times N$ (typically $3 \times N$).

4. Solve
$$\eta W^{EH} \stackrel{l.s.}{=} W^{DB} \tag{7}$$
for the generalized material tensor η; 'l.s.' refers to the least squares solution:
$$\eta = W^{DB} W^{EH+} \tag{8}$$
where '+' indicates the Moore-Penrose pseudoinverse [25]. However, if the number of d.o.f.s M^{EH} is equal to the number of basis modes N, the pseudoinverse turns into a regular inverse.

In contrast with with the procedure published earlier [72], the matrices in (7) are not position-dependent. Another beneficial difference with [72] is that pseudoinversion is no longer needed if W^{EH} is a square matrix.

System (7) defines the generalized material tensor. The structure of this system is shown in Fig. 5. The matrix in the right hand side has, in the general 3D case, six rows corresponding to the six local d.o.f. $\langle D_{x,y,z} \rangle_{\partial\Omega}$ and $\langle B_{x,y,z} \rangle_{\partial\Omega}$. Each column of this matrix corresponds to a basis mode. The entries of the matrix are the mean boundary values of the $\mathbf{D}$ and $\mathbf{B}$ interpolants of the respective mode. The EH-matrix on the left is analogous, except that it may also include nonlocal d.o.f. symbolically indicated as ∂E, ∂H;

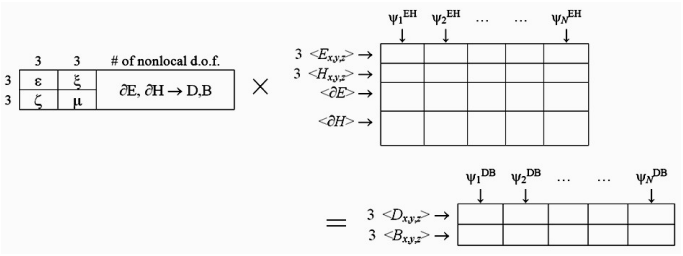

Figure 5: The structure of matrix equations for the material tensor. See text for details.

the number of these nonlocal d.o.f. may vary depending on the desired accuracy of the material model. Finally, the generalized material tensor on the left contains a leading 6×6 block with the standard electromagnetic parameters: the ϵ and μ tensors as well as magnetoelectric coupling parameters ξ and ζ (also in general tensorial). The remaining block, indicated symbolically as $\partial E, \partial H \to D, B$ is novel; it quantifies spatial dispersion as the dependence of fields $\mathbf{D}$ and $\mathbf{B}$ on the *variations* of $\mathbf{E}$ and $\mathbf{H}$ within the cell rather than on their mean values.

F Approximation Errors

With the material tensor rigorously defined, we are in a position to identify clearly the approximations made and the respective errors.

Out-of-the-basis errors δ in (6) is due to the fact that the field in the lattice cell cannot be exactly represented by a finite number of modes.

In-the-basis error γ stems from the least squares fit of the material relation (7). This error can be quantified as
$$\gamma = \|W^{DB} - \eta W^{EH}\| / \|W^{DB}\| \tag{9}$$
where $\|\cdot\|$ is a suitable matrix norm.

There is a trade-off between the two types of error. If a very large set of basis modes in the field expansion is taken, the field can be represented very accurately, and the residual "out-of-the-basis" field can be very small. However, the "in-the-basis" error will tend to increase: it is more difficult to characterize a larger number of modes simultaneously with the same parameter tensor (unless the set of degrees of freedom is also expanded to include a larger number of nonlocal variables). Conversely, if the number of basis modes is smaller, the "in-the-basis" error may decrease (for example, six modes can in general be represented uniquely by a 6×6 tensor containing only local parameters, but seven or more modes in general cannot). However, for a smaller number of modes the out-of-the-basis error can be expected to be higher, unless one is seeking a "customized" set of material parameters tailored just to this specific set of modes.

These two types of error are not exclusive to the proposed methodology. It can be argued that they are present in any rigorous homogenization method, even if not explicitly specified or discussed. Indeed, any serious method must rely on some representation of the field within a lattice cell, and any such representation is by necessity approximate, unless the cell size is vanishingly small. Likewise, the set of material parameters, however defined and computed, must apply to a large variety of excitation conditions and to the

respective field distributions; this again can only be approximate for nonvanishing cell sizes.

In the proposed theory, the errors are clearly and explicitly identified and quantified not only in the asymptotic "big-$\mathcal{O}$" sense but also numerically; see Section V.

IV "Spatial Dispersion:" the Wheat and the Chaff

The goal of this section is to recap the notions of nonlocality / spatial dispersion for natural materials and to see to what extent these notions apply to metamaterials. For brevity of notation, this section deals only with the $(\mathbf{e}, \mathbf{d})$ pair of fields, but similar considerations apply to constitutive relationship between all fields.

Consider first an *infinite homogeneous* medium with a nonlocal spatial response of the form (in the frequency domain)

$$\mathbf{d}(\mathbf{r}) \;=\; \int_{\mathbf{r}'} \epsilon(\mathbf{r}-\mathbf{r}')\,\mathbf{e}(\mathbf{r}')d\mathbf{r}'$$

Dependence of all variables on frequency ω is suppressed to shorten the notation. The integral is taken over the whole space. The Fourier transform simplifies this relationship drastically by turning convolution into multiplication:

$$\mathbf{d}(\mathbf{k}) \;=\; \epsilon(\mathbf{k})\,e(\mathbf{k})$$

However, if the medium is *not* homogeneous in the whole space, the translational invariance is broken and the nonlocal convolutional response becomes a function of two position vectors independently, rather than just of their difference [1, 43]:

$$\mathbf{d}(\mathbf{r}) \;=\; \int \epsilon(\mathbf{r},\mathbf{r}')\,\mathbf{e}(\mathbf{r}')d\mathbf{r}'$$

This expression is no longer simplified by the Fourier transform, and the permittivity can no longer be expressed as a function of a single $\mathbf{k}$-vector in Fourier space.

Since metamaterials are obviously always finite in spatial extent, spatial dispersion in them, strictly speaking, cannot be described by the dependence of effective material parameters (however defined) on a single $\mathbf{k}$-vector. If this limitation is ignored, the practical result is likely to be "smearing" of material characteristics at the material-air interfaces and violation of the Maxwell boundary conditions. This problem can be alleviated by introducing additional surface currents, but separate constitutive relations for such currents are then needed.

Still, in many publications material parameters are derived for a single wave, and then dependence of these parameters on the wavevector $\mathbf{k}$ is investigated. This approach raises further questions, in addition to the lack of translational invariance noted above. First, fundamentally, electromagnetic parameters cannot be defined only from waves propagating in the bulk [72]. This is so because a gauging transformation may change the relationships between the fields while leaving Maxwell's equations unchanged [72, 75]. As a simple example, given the microscopic physical fields $\mathbf{e}$ and $\mathbf{b}$ and the auxiliary fields $\mathbf{d}$ and $\mathbf{h}$, one observes that Maxwell's equations are invariant with respect to the transformation $\mathbf{h}' = \mathbf{h}/2$, $\mathbf{d}' = \mathbf{d}/2$, $\mu' = 2\mu$, $\epsilon' = \epsilon/2$, even though the material parameters have changed by a factor of two. It is through the boundary conditions on the material-air (or material / dielectric) interfaces that the $\mathbf{d}$ and $\mathbf{h}$ fields are gauged uniquely.

Second, a natural definition of material parameters for a single Bloch wave propagating in the bulk of an intrinsically nonmagnetic metamaterial yields only a trivial result for the effective magnetic permeability, and hence artificial magnetism cannot be explained. To elaborate, consider an x-polarized Bloch wave traveling in the z direction (e.g. [70, 69]):

$$\mathbf{e}_B(z) \;=\; E_{\mathrm{PER}}(z)\exp(\mathrm{i}K_B z)\hat{x} \tag{10}$$

$$\mathrm{i}\omega c^{-1}\mathbf{b}_B(z) = \hat{y}(E'_{\mathrm{PER}}(z)+\mathrm{i}K_B E_{\mathrm{PER}}(z))\exp(\mathrm{i}K_B z) \tag{11}$$

Here "PER" indicates a factor periodic over the cell; K_B is the Bloch wavenumber. For this Bloch wave to mimic a plane wave in an equivalent effective medium, one has to have the dispersion relation

$$\omega^2\mu_{\mathrm{eff}}\epsilon_{\mathrm{eff}} \;=\; K_B^2 \tag{12}$$

and the wave impedance

$$(\mu_{\mathrm{eff}}/\epsilon_{\mathrm{eff}})^{\frac{1}{2}} \;=\; \langle e_B\rangle/\langle b_B\rangle \;=\; \omega/K_B \tag{13}$$

where the angle brackets denote an averaging procedure that eliminates the periodic function E'_{PER} and leaves only the dc component in E_{PER}. From the two conditions above, it follows immediately that $\mu_{\mathrm{eff}} = 1$.

Third, even if all the complications above are somehow circumvented, a single Bloch or plane wave still does not carry enough information identifying the whole 6×6 material parameter matrix, so the problem is badly underdetermined. Recognizing that, Fietz & Shvets [21] consider a *collection* of test waves that allow one to set up a system of equations for all parameters. A critique of these approaches can be found in [44] but is not directly relevant in the context of the present paper.

All of this is not to say that "spatial dispersion" is an invalid notion for metamaterials. To the contrary, the theory proposed in this paper does lead to its precise and mathematically quantifiable definition. The message here is that "spatial dispersion" is a loaded expression that should be used with extreme care and with accurate definitions; it cannot be blindly transplanted from the analysis of natural materials to metamaterials. For natural media, the material parameters are *extraneous* to the Maxwell model (they come from measurements supported by analytical and quantum mechanical considerations), so a reasonable particular form of these parameters such as $\epsilon = \epsilon(\mathbf{k})$ can just be postulated. In contrast, the Maxwell model for metamaterials (with given intrinsic characteristics of all natural components involved) is completely self-contained and does not include any extraneous parameters. "Spatial dispersion" in metamaterials will remain a heuristic notion or even a figure of speech unless and until the effective parameters are clearly and rigorously defined. This, in turn, requires a precise definition of the coarse-grained fields.

V Application Examples

A A Single Inclusion with Interior Resonances

This example involves high-permittivity inclusions with strong resonance effects. The setup and parameters are very similar to the ones in [19, 20], where a special asymptotic method was developed and additional adjustable parameters were needed [20]. The methodology of the present paper handles this case with ease and without any additional assumptions or parameters.

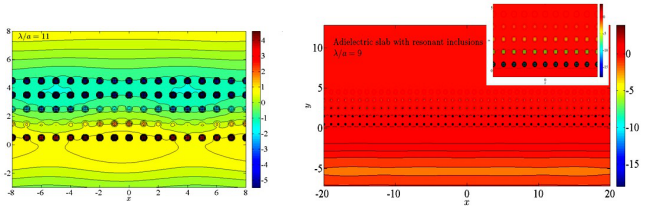

Figure 6: Re(H) in the vicinity of a slab with resonant inclusions; p-mode. Radius of the inclusions relative to the cell size $r/a = 0.25$; their permittivity $\epsilon_{\text{incl}} = 200 + 5\text{i}$ (as in [20]). Left: pass band, $\lambda/a = 11$; right: bandgap, $\lambda/a = 9$; inset: zoom-in on a few cells.

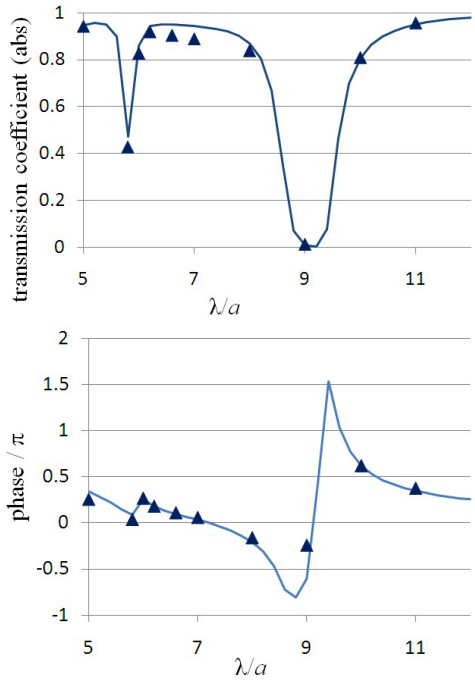

Figure 7: Transmission coefficient (with respect to H) of a five-layer slab as a function of the vacuum wavelength (top: absolute value, bottom: phase). $r/a = 0.25$; $\epsilon_{\text{incl}} = 200 + 5\text{i}$. Triangles: direct finite difference simulation [69]; lines: slab with effective parameters. Normal incidence.

The lattice cell contains a high-permittivity cylindrical inclusion ($\epsilon_{\text{incl}} = 200 + 5\text{i}$); its radius relative to the cell size is $r/a = 0.25$; the normalized vacuum wavelength λ/a varies from 5 to 12. Most interesting is the H-mode (p-mode) where the electric field cuts across the cylinders and strong resonances can be induced.

The effective medium theory developed here agrees very well with "brute force" finite difference simulations where all inclusions are represented directly. As in [72], propagation of waves through a homogeneous "effective parameter" slab is compared with the numerical simulation of this propagation through the actual metamaterial. High-order finite difference "FLAME" schemes ([68, 69, 71] were used for the numerical simulation. Fig. 6 illustrates the distribution of the real part of the magnetic field for normal incidence in the pass band, $\lambda/a = 11$, and in the bandgap, $\lambda/a = 9$.

Fig. 7 demonstrates that the transmission coefficient for the slab with effective parameters is very close, both in the absolute value and phase, to the "true" coefficient from the accurate finite difference simulation.

The in-the-basis error γ (9) is below 10% for $\lambda/a \gtrapprox 5$ and under 5% for $\lambda/a \gtrapprox 9$ (Fig. 8).

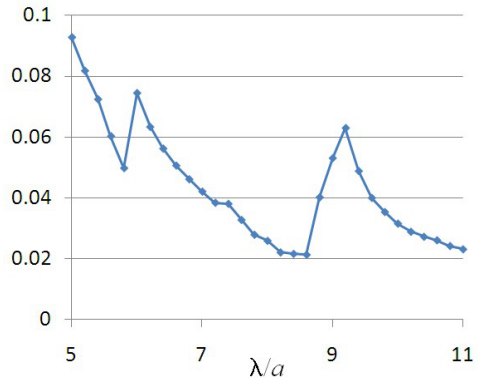

Figure 8: In-the-basis error γ for the metamaterial with resonant inclusions.

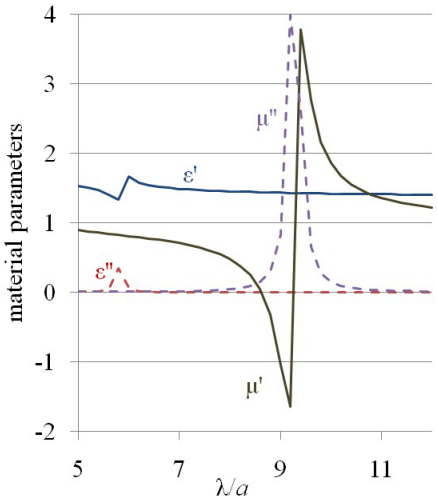

Figure 9: Effective parameters of the metamaterial with resonant inclusions.

The effective parameters plotted in Fig. 9 exhibit a fairly weak electric resonance near $\lambda/a \sim 5.5$ and a strong magnetic resonance around $\lambda/a \sim 9$. As should be expected by symmetry considerations, the magnetoelectric coupling in this example is zero (numerically, it is at the roundoff error level).

B A Particle Trimer with Interior Resonances

A second example involves a trimer of nanoparticles with the same high value of the dielectric permittivity as before, $\epsilon = 200 + 5\text{i}$, but with a twice smaller radius $r/a = 0.125$. The H-mode (TE) is again of greater interest due to the interior resonances in the trimer. The basis functions used in the analysis are eight Bloch waves traveling in the directions $\phi_m = m\pi/4$ ($m = 0, 1, \ldots, 7$) relative to the x-axis. Two such modes, for $\lambda/a = 4.6$ and 8, with $\alpha_m = \pi/4$ are displayed in Fig. 10 as an example.

The choice of the nonlocal degrees of freedom for H comes from the following considerations. The x- and y-derivatives of H are proportional to D_y and D_x and hence (on the boundary) to E_y and E_x, respectively. These d.o.f. would therefore be redundant because the electric field is already included in the local set of d.o.f. With regard to second derivatives, including both $\partial^2 H/\partial x^2$ and $\partial^2 H/\partial y^2$ would be redundant, as the wave equation on the boundary makes the sum of these derivatives proportional to H itself; but

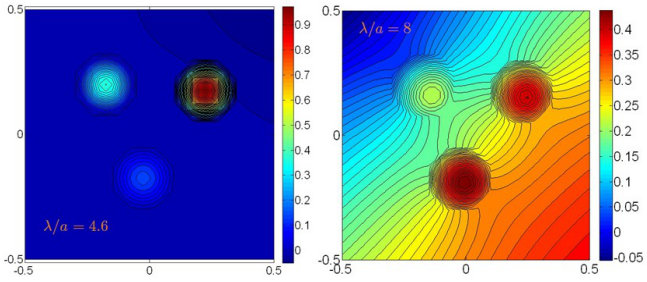

Figure 10: Examples of Bloch modes in a nanoparticle trimer; the real part of H shown. $r/a = 0.125$; $\epsilon_{\text{incl}} = 200 + 5\text{i}$ for all three particles. Left: $\lambda/a = 4.6$; right: $\lambda/a = 8$. The jagged contour lines are only an artifact of grid-based drawing; the FLAME solution [68, 69, 71] itself is very accurate.

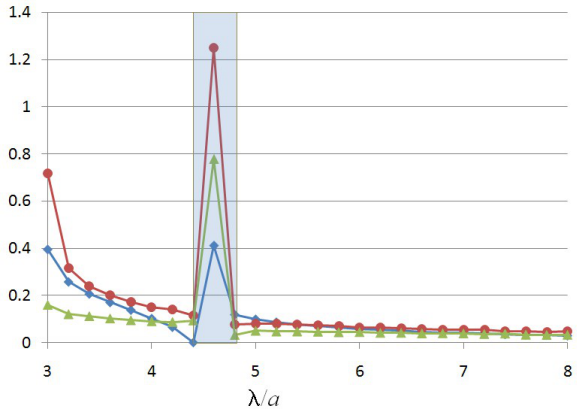

Figure 11: Diamonds: in-the-basis error γ for the particle trimer. Triangles: the matrix norm of column 4 of the material tensor. Circles: same for column 5. (Columns 4 and 5 characterize nonlocal response.)

H is already included as a local d.o.f.

With all this in mind, two nonlocal d.o.f. used for homogenization were $\partial^2 H/\partial x \partial y$ and $(\partial^2 H/\partial x^2 - \partial^2 H/\partial y^2)$. The material tensor in this example is then represented by a 3×5 matrix. Its rows correspond to D_x, D_y and B and its columns 1 through 3 – to E_x, E_y, H. Columns 4 and 5 correspond to the two nonlocal d.o.f. defined above. Note that the use of second derivatives as d.o.f. implies second-order Whitney-like interpolation.

It is instructive to examine the plots of local effective parameters *in conjunction* with the in-the-basis error γ and with the nonlocal parameters (Figs. 11, 12). First, γ increases sharply in the bandgap (shaded areas in the figures). This is to be expected because the *propagating* Bloch waves, used as basis modes in the homogenization procedure, approximate the fields in the bandgap very poorly. This could be rectified by replacing the traveling waves with evanescent ones in the basis, but that is not our primary interest here.

The magnitude of γ is also high (~ 0.4) for $\lambda/a \sim 3$. This implies that the effective parameters for such short wavelengths may be used as qualitative measures at best. The accuracy can be improved by expanding the set of nonlocal d.o.f.; in other words, accuracy can be traded for the level of nonlocality in the material model adopted.

The imaginary parts of ϵ_{xx}, ϵ_{yy} and μ are very close to zero outside the bandgap. Within the gap, their values (including small negative ones) are unreliable because the

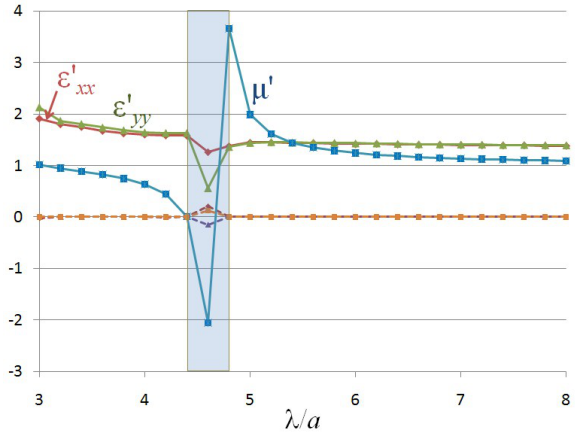

Figure 12: Effective parameters of the particle trimer. Solid lines: real parts. Dashed lines: imaginary parts. Diamonds: ϵ_{xx}; triangles: ϵ_{yy}; squares: μ.

error γ is high. In the wavelength ranges where γ is low or moderate, the local and nonlocal parameters together provide a meaningful characterization of the metamaterial. In particular, the level of spatial dispersion is quantified by the matrix norms of the fourth and fifth columns of the extended material tensor (Fig. 11). From the plots, one may conclude that a purely local model is qualitatively correct for $\lambda/a \gtrapprox 4$ (but outside the bandgap) and quantitatively correct for $\lambda/a \gtrapprox 7$. To turn qualitative analysis into quantitative (say, for $\lambda/a = 3.5$), one needs reliable tools of electrodynamic simulation with nonlocality taken into account. Such tools – currently in their initial stages of development – will be discussed elsewhere.

VI Future Work

The theory proposed here suggests a research program that may progress in several related but diverse directions.

The choice of basis functions. For the sake of brevity and to keep the analysis in focus, the paper deals almost exclusively with Bloch modes as approximating functions for the field in the cell. Propagating Bloch waves are a natural choice for periodic media in the bulk but not for random media and not necessarily in the vicinity of material interfaces. Therefore other possibilities need to be explored. One option is to define the tangential components of the electric or magnetic field on the cell boundary as low order polynomials and to compute the respective basis functions satisfying these boundary conditions. (It is tacitly assumed that the cell boundary does not cut through the microstructure of the cell; otherwise polynomials would not be appropriate.)

The choice of nonlocal degrees of freedom is critical. In the paper, it is made on physical grounds – avoiding redundancy and linear dependence of the local d.o.f. It would be highly desirable to put this on a more solid mathematical ground.

Numerical methods for nonlocal models. Weak nonlocality will result either in differential equations of higher order or, alternatively and preferably, in integrodifferential equations. In the latter case, the inte-

gral kernels will have a small support if the nonlocality is weak, so the computational cost will be reasonable; however, new computational methods will still be needed to handle such problems.

Energy-based approaches. The methodology of this paper defines effective parameters by relating face fluxes of $(\mathbf{d}, \mathbf{b})$ to the edge circulations of $(\mathbf{e}, \mathbf{h})$. Alternatively, one can define these parameters by equating the energies on the microscopic and coarse-grained levels. This idea, suggested to me by several colleagues [24, 30, 59], is closely related to Hiptmair's work on discrete Hodge operators [28] but has not yet been implemented, except for a toy 1D problem.

Random media. The methodology has been applied only to periodic structures so far. The key ideas should remain valid for random media as well, but many elements of the procedure will need to be worked out afresh.

Mathematical foundation. The material in this paper is presented at the "engineering level" of rigor. A more formal mathematical foundation, with a functional-analytic setup and convergence proofs, would definitely be desirable and could be based on the theory of discrete Hodge operators [28]. As always, convergence properties of a model depend on its consistency and stability. It is fairly straightforward to demonstrate that the consistency error of the proposed homogenization model corresponds to the approximation accuracy of the chosen basis set. Stability is more difficult to establish rigorously.

Applications. In photonics, there are abundant applications of effective parameter models for metamaterials, particle and hole [26] arrays. Beyond photonics, homogenization of laminated stator cores of electric machines springs to mind [13, 27]. The method can be extended beyond electromagnetics as well, to acoustics, heat transfer and possibly to problems of elasticity.

Time will tell which of these directions are more fruitful.

VII Conclusion

The proposed homogenization theory unifies local and nonlocal material parameters in an extended tensor. The leading block (6×6 in the general case of 3D electrodynamics) of this tensor relates the mean values of the coarse-grained $(\mathbf{E}, \mathbf{H})$ and $(\mathbf{D}, \mathbf{B})$ pairs and contains the standard set of parameters: the permittivity and permeability tensors, as well as the magnetoelectric coupling if present. The nonlocal block of the extended tensor relates the mean values of $(\mathbf{D}, \mathbf{B})$ to the variations / derivatives of $\mathbf{E}, \mathbf{H}$. By expanding the set of nonlocal degrees of freedom, one can increase the accuracy of the material model at the expense of its higher complexity (higher level of nonlocality). In principle, there is a quasi-continuous spectrum of models, from local ones with a small number of d.o.f. (up to 36) to nonlocal ones and to fully numerical ones (a very large number of d.o.f. for the latter). This point of view unifies local, nonlocal and numerical treatment of metamaterials.

The consolidation of local and nonlocal parameters in the generalized tensor suggests that all these parameters are interrelated. This puts into a proper perspective, for example, the recent experimental work of Gompf *et al.* showing that spatial dispersion can mimic chirality [23, 26].

The theory of this paper stems from a small number of fundamental principles – most importantly, that the coarse-grained fields must satisfy Maxwell's equations and boundary conditions and that material parameters are, by definition, linear maps between the (pairs of) coarse-grained fields. Consequently, the **E** and **H** fields are produced by an interpolation that preserves tangential continuity (see Section III and [72]), while for **D** and **B** normal continuity is maintained.

Two types of approximation errors are clearly identified. (These errors are not exclusive to the proposed methodology and are present in any rigorous homogenization procedure.) The first type ("out-of-the-basis" error) is due to the fact that the field in a finite-size lattice cell has infinitely many degrees of freedom and cannot be exactly represented by a finite number of modes. The second type ("in-the-basis" error) is due to the fact that a large number of different modes cannot in general conform to a smaller number of material parameters. Ways of reducing these errors are identified.

The proposed theory does not involve any heuristic assumptions or artificial averaging rules. The effective parameters are defined directly via field analysis in the lattice cell, in contrast with methods where these parameters are obtained from reflection/transmission data or other indirect considerations. Nontrivial magnetic behavior, if present, follows logically from the method. Illustrative examples of resonant structures are presented.

Acknowledgment

I thank Vadim Markel, Dmitry Golovaty, Graeme Milton, Boris Shoykhet, Sergey Bozhevolnyi and Ralf Hiptmair for very helpful and insightful comments and conversations. I am grateful to Anders Pors for implementing the method in 3D [54] and for asking pointed questions that helped to crystallize the ideas of the present paper. Special thanks to Ralf Vogelgesang and Bruno Gompf for a very detailed discussion of their recent experimental work in connection with the proposed theory.

VIII References

[1] V. M. Agranovich and V. L. Ginzburg. *Crystal Optics with Spatial Dispersion, and Excitons.* Berlin; New York: Springer-Verlag, 2nd ed. (1984).

[2] I. Babuška and J.M. Melenk. The partition of unity method. Int. J. for Numer. Meth. in Eng., **40**(4):727–758 (1997).

[3] Ivo Babuška and Robert Lipton. Optimal local approximation spaces for generalized finite element methods with application to multiscale problems. Multiscale Modeling and Simulation, SIAM **9**:373-406 (2011).

[4] N. S. Bakhvalov and G. Panasenko. *Homogenisation: Averaging Processes in Periodic Media, Mathematical Problems in the Mechanics of Composite Materials.* Springer (1989).

[5] A. Bensoussan, J.L. Lions, and G. Papanicolaou. *Asymptotic Methods in Periodic Media.* North Holland, 1978.

[6] A. Bossavit. Whitney forms: A class of finite elements for three-dimensional computations in electromagnetism. IEE Proc. A, **135**:493–500 (1988).

[7] Alain Bossavit. *Computational Electromagnetism: Variational Formulations, Complementarity, Edge Elements.* San Diego: Academic Press (1998).

[8] A. Bossavit, G. Griso, B. Miara. Modelling of periodic electromagnetic structures bianisotropic materials with memory effects. J. Math. Pures & Appl. **84**(7):819–850 (2005).

[9] Wenshan Cai, Uday K. Chettiar, Hsiao-Kuan Yuan, Vashista C. de Silva, Alexander V. Kildishev, Vladimir P. Drachev, and Vladimir M. Shalaev. Metamagnetics with rainbow colors. Optics Express, **15**(6), 3333–3341 (2007).

[10] X. Chen, T. M. Grzegorczyk, B.-I. Wu, J. Pacheco, and J. A. Kong, Robust method to retrieve the constitutive effective parameters of metamaterials, Phys. Rev. E **70**, 016608 (2004).

[11] X. Chen, B.-I. Wu, J. A. Kong, and T. M. Grzegorczyk, Retrieval of the effective constitutive parameters of bianisotropic metamaterials, Phys. Rev. E **71**, 046610 (2005).

[12] Tuck C. Choy. *Effective Medium Theory: Principles and Applications.* Oxford University Press (1999).

[13] Stphane Clénet, private communication, 2011.

[14] Carl de Boor. Divided differences. Surv. Approx. Theory **1**:46–69 (2005).

[15] G. Dal Maso, An introduction to Γ-convergence, Birkhauser (1992).

[16] James W. Demmel. Applied Numerical Linear Algebra. SIAM (1997).

[17] Weinan E, Bjorn Engquist, Xiantao Li, Weiqing Ren, Eric Vanden-Eijnden. Heterogeneous multiscale methods: A review. Comm Comp Phys **2**(3):367–450 (2007).

[18] B. Engquist, O. Runborg. Projection generated homogenization. In: N. Antonic, C.J. VanDuijn, W. Jager, A. Mikelic (eds), *Multiscale Problems in Science and Technology: Challenges to Mathematical Analysis and Perspectives*, 129–150 (2000).

[19] D. Felbacq, G. Bouchitté. Theory of mesoscopic magnetism in photonic crystals. Phys Rev Lett, **94**:183902 (2005).

[20] D. Felbacq, B. Guizal, G. Bouchitté, C. Bourel. Resonant homogenization of a dielectric metamaterial. Microwave and Opt Tech Lett **51**:2695–2701 (2009).

[21] Chris Fietz and Gennady Shvets. Current-driven metamaterial homogenization. *Physica B: Cond Mat* **405**(14), 2930–2934 (2010).

[22] J. Fish, V. Belsky. Multigrid method for periodic heterogeneous media. 2. Multiscale modeling and quality-control in multidimensional case. Comp Meth Appl Mech Eng **126**(1-2):17–38 (1995).

[23] Bruno Gompf and Ralf Vogelgesang, private communication (2011).

[24] Dmitry Golovaty, private communication (2010–2011).

[25] Gene H. Golub and Charles F. Van Loan. *Matrix Computations.* The Johns Hopkins University Press: Baltimore, MD (1996).

[26] Bruno Gompf, Julia Braun, Thomas Weiss, Harald Giessen, Martin Dressel and Uwe Hübner. Periodic nanostructures: Spatial dispersion mimics chirality. Phys. Rev. Lett. **106**, 185501 (2011).

[27] J. Gyselinck, P. Dular. A time-domain homogenization technique for laminated iron cores in 3-D finite-element models. IEEE Trans Magn **40**(2):856–859 (2004).

[28] R. Hiptmair. Discrete Hodge operators. Numerische Mathematik **90**(2):265–289 (2001).

[29] R. Hiptmair, A. Moiola and I. Perugia. Error analysis of Trefftz-discontinuous Galerkin methods for the time-harmonic Maxwell equations, Preprint IMATI-CNR Pavia, 5PV11/3/0, http://www-dimat.unipv.it/perugia/preprints/tdgm.pdf (2011).

[30] Ralf Hiptmair, private communication (2011).

[31] Thomas Y. Hou and Xiao-Hui Wu. A multiscale finite element method for elliptic problems in composite materials and porous media. J Comp Phys **134**:169-189 (1997).

[32] Thomas Y. Hou, Xiao-Hui Wu, Zhiqiang Cai. Convergence of a multiscale finite element method for elliptic problems with rapidly oscillating coefficients. Math of Comp, **68**(227):913–943 (1999).

[33] V.V. Jikov, S.M. Kozlov, O.A. Oleinik. *Homogenization of Differential Operators and Integral Functionals.* Springer-Verlag: Berlin ; New York (1994).

[34] L. Kettunen, K.Forsman, A.Bossavit. Discrete spaces for div and curl-free fields. IEEE Trans Magn **34**(5):2551–2554 (1998).

[35] N. A. Khizhnyak, Artificial anisotropic dielectrics: I., Sov. Phys. Tech. Phys. **27**, 2006–2013 (1957). Artificial anisotropic dielectrics: II., ibid. 2014–2026; Artificial anisotropic dielectrics: III., ibid., 2027–2037 (1957).

[36] N. A. Khizhnyak, Artificial anisotropic dielectrics formed from two-dimensional lattices of infinite bars and rods, Sov. Phys. Tech. Phys. **29**, 604–614 (1959).

[37] Peter Robert Kotiuga. *Hodge Decompositions and Computational Electromagnetics.* PhD thesis, McGill University, Montreal, Canada (1985).

[38] D.-H. Kwon, D. H. Werner, A. V. Kildishev, and V. M. Shalaev, Material parameter retrieval procedure for general bi-isotropic metamaterials and its application to optical chiral negative-index metamaterial design, Opt. Express **16**, 11822 (2008).

[39] L.D. Landau and E.M. Lifshitz. *Electrodynamics of Continuous Media.* Oxford; New York: Pergamon (1984).

[40] L. Lewin, The electrical constants of a material loaded with spherical particles. Proc. Inst. Elec. Eng. **94**, 65–68 (1947).

[41] Z. Li, K. Aydin, and E. Ozbay, Determination of the effective constitutive parameters of bianisotropic metamaterials from reflection and transmission coefficients, Phys. Rev. E **79**, 026610 (2009).

[42] Ruopeng Liu, Tie Jun Cui, Da Huang, Bo Zhao, and David R. Smith. Description and explanation of electromagnetic behaviors in artificial metamaterials based on effective medium theory. Phys. Rev. E **76**, 026606 (2007).

[43] Vadim A. Markel. Private communication (2010–2011).

[44] Vadim A. Markel. On the current-driven model in the classical electrodynamics of continuous media. J Phys: Cond Mat, **22**(48):485401 (2010).

[45] Roberto Merlin. Metamaterials and the LandauLifshitz permeability argument: Large permittivity begets high-frequency magnetism. PNAS **106**(6):1693–1698 (2009).

[46] Graeme Milton. *The Theory of Composites*. Cambridge University Press: Cambridge ; New York (2002).

[47] P. B. Ming, X. Y.Yue. Numerical methods for multiscale elliptic problems. J Comp Phys **214**(1):421–445 (2006).

[48] Peter Monk. *Finite Element Methods for Maxwell's Equations*. Oxford: Clarendon Press (2003).

[49] A. Moroz. Effective medium properties, mean-field description, homogenization, or homogenisation of photonic crystals. http://www.wave-scattering.com/pbgheadlines.html

[50] N. Neuss, W. Jager, G. Wittum. Homogenization and multigrid. Computing **66**(1):1–26 (2001).

[51] Jean-Claude Nédélec. Mixed finite elements in $\mathbb{R}^3$. *Numer. Math.*, **35**:315–341 (1980).

[52] Jean-Claude Nédélec. A new family of mixed finite elements in $\mathbb{R}^3$. *Numer. Math.*, **50**:57–81 (1986).

[53] A. Plaks, I. Tsukerman, G. Friedman, and B. Yellen. Generalized Finite Element Method for magnetized nanoparticles. IEEE Trans. Magn., **39**(3):1436–1439 (2003).

[54] Anders Pors, Igor Tsukerman, Sergey I. Bozhevolnyi. Effective constitutive parameters of plasmonic metamaterials: Homogenization by dual field interpolation. Phys Rev E, 016609 (2011).

[55] E. Sanchez-Palencia. *Non-homogeneous Media and Vibration Theory*. Springer Verlag (1980).

[56] A. K. Sarychev and V. M. Shalaev. *Electrodynamics of Metamaterials*. World Scientific, Singapore (2007).

[57] C. Scheiber, A. Schultschik, O. Bíró, R.Dyczij-Edlinger. A model order reduction method for efficient band structure calculations of photonic crystals, IEEE Trans Magn, **47**(5), 1534–1537 (2011).

[58] Jonathon Shlens. A tutorial on principal component analysis, http://www.snl.salk.edu/∼shlens/pca.pdf (2009).

[59] Boris Shoykhet, private communication (2010–2011).

[60] C. R. Simovski. On material parameters of metamaterials (review). Opt & Spectr, **107**:726–753 (2009).

[61] C. R. Simovski and S. A. Tretyakov. On effective electromagnetic parameters of artificial nanostructured magnetic materials. Photonics & Nanostr, **8**:254–263 (2010).

[62] Daniel Sjöberg, Christian Engstrom, Gerhard Kristensson, David J. N. Wall, and Niklas Wellander. A Floquet–Bloch decomposition of Maxwell's equations applied to homogenization. Multiscale Modeling & Simulation, **4**(1):149–171 (2005).

[63] D. R. Smith, S. Schultz, P. Markoš, and C. M. Soukoulis, Determination of effective permittivity and permeability of metamaterials from reflection and transmission coefficients, Phys. Rev. B **65**, 195104 (2002).

[64] David R. Smith and John B. Pendry. Homogenization of metamaterials by field averaging. J. Opt Soc. Am B, **23**(3):391–403 (2006).

[65] D. Stroud. Generalized effective-medium approach to the conductivity of an inhomogeneous material. Phys. Rev. B **12**(8):3368-3373 (1975).

[66] Luc Tartar. *The General Theory of Homogenization: A Personalized Introduction*. Springer (2009).

[67] E. Tonti. A mathematical model for physical theories. Rend. Acc. Lincei, LII, Part I & II:175–181 & 350–356 (1972).

[68] I. Tsukerman. A class of difference schemes with flexible local approximation. J. Comput. Phys., **211**(2):659–699 (2006).

[69] Igor Tsukerman. *Computational Methods for Nanoscale Applications: Particles, Plasmons and Waves*. Springer (2007).

[70] Igor Tsukerman. Negative refraction and the minimum lattice cell size. J. Opt. Soc. Am. B, **25**:927–936 (2008).

[71] I. Tsukerman and F. Čajko. Photonic band structure computation using FLAME. IEEE Trans Magn, **44**(6):1382–1385 (2008).

[72] Igor Tsukerman. Effective parameters of metamaterials: a rigorous homogenization theory via Whitney interpolation. J Opt Soc Am B, **28**:577–586 (2011).

[73] Igor Tsukerman. Nonlocal homogenization of metamaterials by dual interpolation of fields. J Opt Soc Am B, accepted.

[74] J. van Welij. Calculation of eddy currents in terms of H on hexahedra. IEEE Trans Magn, **21**(6):2239–2241 (1985).

[75] A. P. Vinogradov. On the form of constitutive equations in electrodynamics. Phys. Usp., **45**:331-338 (2002).

[76] P. C. Waterman and N. E. Pedersen, Electromagnetic scattering by periodic arrays of particles, J. Appl. Phys. **59**, 2609–2618 (1986).

[77] Niklas Wellander and Gerhard Kristensson. Homogenization of the maxwell equations at fixed frequency. SIAM J. Appl. Math. **64**(1):170-195 (2003).

[78] H. Whitney. *Geometric Integration Theory*. Princeton, NJ: Princeton Univ. Press (1957).

Dedication

This paper is dedicated to the memory of Doug Lavers, who died in a tragic canoe accident in Northwest Canada on July 11, 2011. I have always admired Doug's rare combination of intellect, integrity and good humor. I will miss him greatly and will always remember with fondness the years when we worked together at the University of Toronto. Doug was a wonderful colleague and a wonderful man, always thoughtful, always candid, always friendly, always gracious. May he rest in peace.

Author's name and Affiliation

Igor Tsukerman, Department of Electrical and Computer Engineering, The University of Akron, OH 44325–3904, USA.

igor@uakron.edu